journal of the mechanical behavior of biomedical materials 124 (2021) 104837

Contents lists available at ScienceDirect

Journal of the Mechanical Behavior of Biomedical Materials

journal homepage: www.elsevier.com/locate/jmbbm

Research Paper

A novel multi-structural reinforced treatment on Ti implant utilizing a combination of alkali solution and bioactive glass sol

Mahdis Nesabi [a], Alireza Valanezhad [a,*], Sirus Safaee [a], Tetsurou Odatsu [b], Shigeaki Abe [a], Ikuya Watanabe [a]

[a] Department of Dental and Biomedical Materials Science, Graduate School of Biomedical Sciences, Nagasaki University, 1-7-1 Sakamoto, Nagasaki, 852-8588, Japan
[b] Department of Applied Prosthodontics, Institute of Biomedical Sciences, Nagasaki University, 1-7-1, Sakamoto, Nagasaki, 852-8588, Japan

ARTICLE INFO

Keywords:
Titanium
Bioactive glass
Alkali treatment
Combined coating
Surface

ABSTRACT

Objective: Alkali treatment and bioactive glass (BG) sol dip-coating are well-known individual methods for titanium (Ti) surface modification. In this study, a unique combination of alkali treatment and bioactive glass sol dip coating was applied to the Ti substrate, then the mechanical properties and cell responses were investigated.
Methods: Based on the methods introduced above, the Ti substrate was treated by 6 mL of an NaOH 5 M aqueous solution for 24 h at 60° C; this was followed by adding 1.2 mL of a BG 58S sol to form a novel combined nanostructure network covered by a thin BG layer. For the assessment of the formed coating layer, the morphology, elemental analysis, phase structure, adhesion property and the cell response of the untreated and treated surfaces were investigated.
Results: The BG coating layer was reinforced by the nanostructure, fabricated through the alkali treatment. The results obtained by applying the combined modification method confirmed that the mechanical and biological properties of the fabricated surface demonstrated the highest performance compared to that of the unmodified and individually modified surfaces.
Significance: The achieved upgrades for this method could be gained from the demanded porous nanostructure and the apatite transformation ability of the alkali treatment. Therefore, the hybridized application of the alkali-BG treatment could be introduced as a promising surface modification strategy for hard-tissue replacement applications.

1. Introduction

Titanium (Ti) and its alloys are generally used to replace or augment the hard tissues of the human's body because they demonstrate excellent mechanical properties and osteoinductivity (Khorasani et al., 2015; Gepreel and Niinomi, 2013). Despite these positive qualities, a direct bone connection of Ti is still challenging in clinical applications due to its bioinert surface behavior (Oshida, 2010; Geetha et al., 2009). Furthermore, the bioinert nature of the Ti substrate can cause an inflammatory reaction through the Ti ion release toward the body (Singh and Dahotre, 2007; (Ren et al., 2013); also, its surface still needs to be transferred from a bioinert one to a bioactive one. To tackle these disadvantages, chemical modification of the Ti substrate has been developed. In this regard, fabrication of a bioactive coating layer or a physical modification technique such as inducing roughness to the surface has played a vital role in modifying Ti-based implants (Valanezhad et al., 2012); Mendonça et al., 2008; Mendes et al., 2007; Ponsonnet et al., 2003; Davies et al., 2013; (Le Guéhennec et al., 2007); (Gittens et al., 2011); He et al., 2009; Liu et al., 2004). Kim et al. in 1997 proved that to fabricate a nanostructure coating layer on the Ti substrate with the capability of bone-like apatite transformation and the desired bone-bonding ability, the well-arranged NaOH solution has the best potential and efficiency (HM Kim et al., 1997) to promote mineralization and bone formation (Conforto et al., 2008; Camargo et al., 2017). Nevertheless, individual alkali treatment utilizing NaOH solution builds a permeable layer of titanate which releases Na^{+} and raises the local pH immediately after exposure in biological environments, thus declining the living cells' activity (Li et al., 2014). As another treatment solution, bioactive glass (BG), which was introduced by Larry Hench for the first time (Hench et al., 1971), and the sol-gel derived BG 58S were reported

* Corresponding author. Department of Dental and Biomedical Material Sciences, Graduate School of Biomedical Sciences Nagasaki University, 1-7-1 Sakamoto, Nagasaki, 852-8588, Japan.
E-mail address: vala@nagasaki-u.ac.jp (A. Valanezhad).

https://doi.org/10.1016/j.jmbbm.2021.104837
Received 18 June 2021; Received in revised form 9 September 2021; Accepted 12 September 2021
Available online 15 September 2021

by Li et al. (1991). To begin, BG 58S (58% SiO_2, 38% CaO, 4% P_2O_5) has substantial superiorities, such as bioactivity, bone regeneration ability, biodegradability and direct bone contact (Moghanian et al., 2021d; Chen et al., 2018; Rahmani et al., 2021). In addition, BG 58S, as a coating material with the desired percentage of its components, can play a key role in improving the biological properties of the Ti substrate (Moritz et al., 2004b) (Moghanian et al., 2021c). The bioactivity of the BG coating could be due to the calcium and phosphorus release (Houreh et al., 2017; Gentleman et al., 2010). Furthermore, since the molecular ratios of calcium oxides and phosphorus in BG are similar to that of the natural bone, BG can bind to the mineralized bone and it can therefore be able to increase the biological behavior of the modified substrate, such as ALP activity and the cell proliferation (Moghanian et al., 2021a). Moreover, some recent studies have confirmed that BG with suitable bioactive characteristics can also be incorporated in some other endodontic implants (Vallittu et al., 2018) and biocompatible materials to build a desirable scaffolding system suitable for biomedical applications (Saatchi et al., 2021; Zohourfazeli et al., 2021; Moghanian et al., 2021e); the sol-gel procedure is a well-known method with a low cost and high purity, as compared to other methods. This method is also environmentally safe and homogeneous; it is carried out at room temperature too (Moghanian et al., 2021a, 2021b). Further, the sol-gel preparation technique of BG 58S is quick and straightforward, with remarkable biological properties (Safaee et al., 2021; Bui and Dang, 2019; Moghanian et al., 2021b). The individual BG coated Ti surface demonstrates weaker strength compared to that of the uncoated Ti surface (Schrooten and Helsen, 2000). So, to compensate for such drawbacks, one solution was that by adding the BG 58S sol to the alkali solution after the nanostructure formation, depending on NaOH, a reinforced thin BG 58S coating layer with a homogeneous distribution could be formed on the Ti surface. In the current research, for the first time, the medical grade Ti surface was applied to both afore-mentioned substrate modification techniques, i.e. alkali treatment (NaOH) and BG 58S (SiO_2–CaO–P_2O_5) porous nanocomposite coating. The hypothesis was that by employing the novel combined alkali-BG treatment, the Ti substrate would benefit from the characteristics of both alkali treatment (appropriate porosity, nanostructure network and firmly adhered coating layer) and nanoceramic coating (apatite transformation ability, and desired bioactivity and biocompatibility). Therefore, we aimed to fabricate a high quality BG 58S solution by utilizing the sol-gel method for the first time; then the obtained BG sol was directly added into the NaOH solution containing Ti samples. The hybridized coating layer was then characterized and investigated in terms of bond strength and its biological behavior.

2. Materials and methods

2.1. Materials

The substrates utilized in the current study included medical-grade pure Ti (Nippon Steel & Sumikin Stainless Steel Corp, Tokyo, Japan), sodium hydroxide (NaOH; FUJIFILM Wako Pure Chemical Corporation, Japan), ethyl tetraethyl orthosilicate (TEOS; FUJIFILM Wako Pure Chemical Corporation, Japan), triethyl phosphate (TEP; FUJIFILM Wako Pure Chemical Corporation, Japan), calcium nitrate tetrahydrate ($Ca(NO_3)_2 \cdot 4H_2O$; FUJIFILM Wako Pure Chemical Corporation, Japan), hydrochloric Acid (HCl; FUJIFILM Wako Pure Chemical Corporation, Japan), alpha-minimum essential medium (α.MEM; GIBCO, Invitrogen TM, NY, USA), fetal bovine serum (FBS; GIBCO, Grand Island, NY, USA), 2-phospho-L-ascorbic acid (Asc; SIGMA-ALDRICH, Germany), β-Glycerophosphate disodium salt hydrate (β-Gly; SIGMA-ALDRICH, USA), dexamethasone (Dex; SIGMA-ALDRICH, USA), Alizarin red S staining (SIGMA-ALDRICH Co., St. Louis, MO, USA), alkaline phosphatase (ALP) activity kit (LabAssay™ ALP, FUJIFILM Wako Pure Chemical Industries, Ltd), MTS assay kit (CellTiter 96® AQueous One Solution, Promega, Madison, WI, USA), and preosteoblast cell-line MC3T3-E1 (Riken Cell Bank, Tokyo, Japan).

2.2. Methods

2.2.1. Sample preparation

Pure Ti plates with the diameter of 12 mm and thickness of 1 mm were divided into four groups and then applied to prepare the designed modified surfaces in this study. The substrates were all polished by waterproof SiC polish papers with 400# grits. The ground substrates were then washed with acetone, ethanol and deionized water using an ultrasonic cleaner (VS–F100, As One Corp, Osaka, Japan) for 15 min each. The washed samples were then dried in an oven (D0450FA, As One Corp, Osaka, Japan) at 37 °C for 1 h and used as the control samples (named Ti).

2.2.2. Alkali treatment

Alkali treated Ti (Ti-A) substrates were produced by immersing the Ti samples into 6 mL of the NaOH (5 M) solution in polypropylene tubes; the tubes were then placed in an oil bath shaker (SB-13, AS ONE, Osaka, Japan) at 60 °C for 24 h. The alkali-treated samples were rinsed with deionized water for 30 s and dried at 37 °C for 12 h.

2.2.3. Preparation of the BG 58S sol

The BG-coated Ti substrates (Ti-BG) were fabricated by applying the sol dip-coating method. The BG 58S sol was derived from the sol-gel method; accordingly, 10.24 gr TEOS, 1.16 gr TEP, 7.02 gr ($Ca(NO_3)_2.4H_2O$), 1.30 gr Hydrochloric Acid (2 M), and 7.82 gr deionized water were mixed and stirred using a magnetic stirrer (HS–360H, As One Corp, Osaka, Japan) with 600 rpm for 3 h to form a clear and uniform sol (Chen et al., 2018). The Ti substrates were coated by the sol dip-coating method under the following conditions: dip length: 60 mm, dip speed: 9 mm/s, return speed: 9 mm/s, dip duration: 4 s, and dry duration: 60 s. The coating procedure was followed with heating at 650 °C for 1 h (Safaee et al., 2021).

2.2.4. Combination treatment of Alkali-BG

The combined BG-coated alkali-treated Ti substrates (Ti-A-BG) were produced by a unique hybrid method. In this method, Ti substrates were soaked into 6 mL of the NaOH (5 M) solution in polypropylene tubes; the tubes were then placed in an oil bath shaker at 60 °C for 24 h; after the alkali treatment, the BG sol was added to the NaOH with the ratio of 1/5. The samples were kept in the treatment tube containing the mixed solution at 60 °C for 1 h inside the shaker. The Ti-A-BG samples were then rinsed with deionized water and this was followed by heating at 650 °C for 1 h.

2.2.5. Characterization studies

The coated substrates' surface morphology in various conditions was observed by scanning electron microscopy (SEM: JEOL, JCM-6000 Plus, Tokyo, Japan) at the accelerating voltage of 15 kV after the conventional gold sputtering. The chemical composition and elemental analyses of the coating layer were analyzed using energy-dispersive X-ray spectroscopy (EDS, FE-SEM: JSM-7500, JEOL, Tokyo, Japan). The phase structure of the coated layer on the substrate, before and after treatment, was analyzed by an X-ray diffractometer (XRD) (Miniflex600, Rigaku co, Tokyo, Japan). The diffractometer operated at 40 kV and 15 mA, with a 2θ range of 20–80°, by utilizing a step size of 0.02.

2.2.6. Adhesion test

The adhesive strength of the Ti, Ti-A, Ti-BG and Ti-A-BG substrates was tested using a universal testing machine (Instron 5566S, Canton, MA, USA). The test was carried out by the method shown in Fig. 1. The aluminum stud-pins with the diameter of 2.7 mm, were covered by a reinforced epoxy resin adhesive (ROMULUS IV, Epoxy Resin Adhesive, Quad Group, Spokane, WA, USA) with the thickness of 50 μm; they were clipped on the center of the Ti samples surface and heated at 150 °C for 1 h to attach the pins to the sample. The heated samples and pins were then slowly cooled to room temperature until the resin was completely

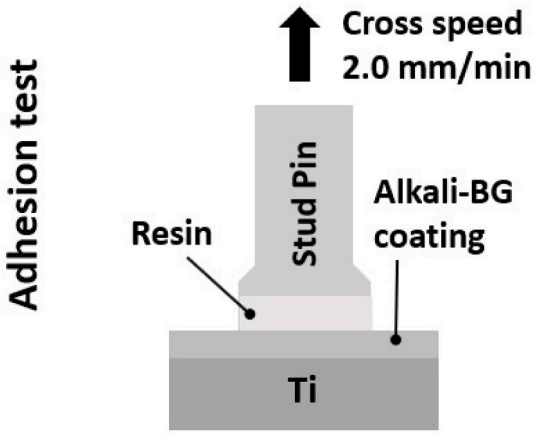

Fig. 1. Schematic illustration of the adhesion test.

hardened. The samples were then placed on the universal testing machine and the stud pins were pulled under a crosshead speed of 2 mm/min until the bonding between the coating and stud pin was destroyed. The measurement was repeated two times for eight similar surfaces in the four mentioned separate groups. Finally, the standard deviations and average adhesive strength values of the data obtained were calculated.

2.2.7. Cell response

The *in vitro* cell response of the substrates was investigated using MC3T3-E1 cells. The cells were cultured in a plain medium containing an α.MEM supplemented with 10% FBS, 100 units/mL penicillin and 100 μg/mL streptomycin; this was in a humidified 5% CO_2 balanced-air incubator at 37 °C. A differentiation medium was prepared by applying 50 mL FBS, 50 μg/mL Asc, 10 m*M* β-Gly, and 50 n*M* Dex to the plain medium. For the viability test, the mitochondrial dehydrogenase activity of the specimens was measured by the MTS assay. The samples were divided into four experimental groups: Ti (control), Ti-A, Ti-BG, and Ti-A-BG (n = 8). They were then placed in the cell culture plates; the MC3T3-E1 cells were seeded onto the samples. Cell density was 2×10^4 cells/mL and incubation was done at 37 °C with 5% CO_2. The medium was changed every two days. The viability of the samples was evaluated after 2, 4 and 6 days; this was followed by the incubation of the cells for 4 h. The absorbance was measured using a plate reader (Multiskan™ FC, Thermo Fisher Scientific, Waltham, MA, USA) at the wavelength of 492 nm.

Differentiation of the cells on the substrates was assessed by determining the ALP activity. Cells were cultured on the specimens per group for the differentiation test (n = 8). The ALP activity was examined after 3, 7, 14 and 21 days of incubation. The cells were denatured in an extraction solution for 15 min; the substrate solution was also added and kept for 45 min; this was followed by adding the stop solution as a final step. The obtained solution was transferred to 96 well plates and the absorbance was measured using a plate reader at the wavelength of 405 nm to evaluate cells differentiation. Calcified nodule formation and mineralized matrix formation of the specimens were evaluated using Alizarin red S staining method. After each incubation period, including 3, 7, 14 and 21 days, the samples were washed twice with PBS and stained in 5% Alizarin red S for 15 min. The staining solution was aspirated, and the stained samples were washed with deionized water to remove the excess staining reagent. The stained samples were then observed using digital microscopy (VHY–100K, Keyence, Tokyo, Japan).

Statistical analysis was carried out by using a one-way analysis of variance (ANOVA) with the statistical significance set at $P < 0.05$ (*) and $P < 0.01$ (**).

3. Results

3.1. Characterization of the modified substrates

Fig. 2 shows the SEM images of the untreated and treated Ti surfaces in various treatment conditions. The SEM image of the Ti substrate is presented in Fig. 2(a, A) as a control sample. Fig. 2(b, B) also exhibits the surface morphology of the alkali treated substrate, Ti-A, with a nanostructure formed on its surface by alkali treatment. Further, Fig. 2(c, C) shows the BG 58S coated substrate and Ti-BG substrate's morphology. As it can be seen that a relatively non-homogeneous distribution of the BG particles was formed after coating with the BG 58S. Fig. 2(d, D) exhibits the substrate subjected to the combined alkali-BG treatment method (Ti-A-BG). The Ti-A-BG substrate's surface showed a fully covered homogeneous coating layer containing a uniform distribution of BG 58S nanoparticles on the porous nanostructure network.

Fig. 3 demonstrates the FE-SEM micrographs and the EDS elemental analyses of the Ti, Ti-A, Ti-BG, and Ti-A-BG substrates. Fig. 3(a) also shows the untreated Ti morphology and the EDS elemental analysis

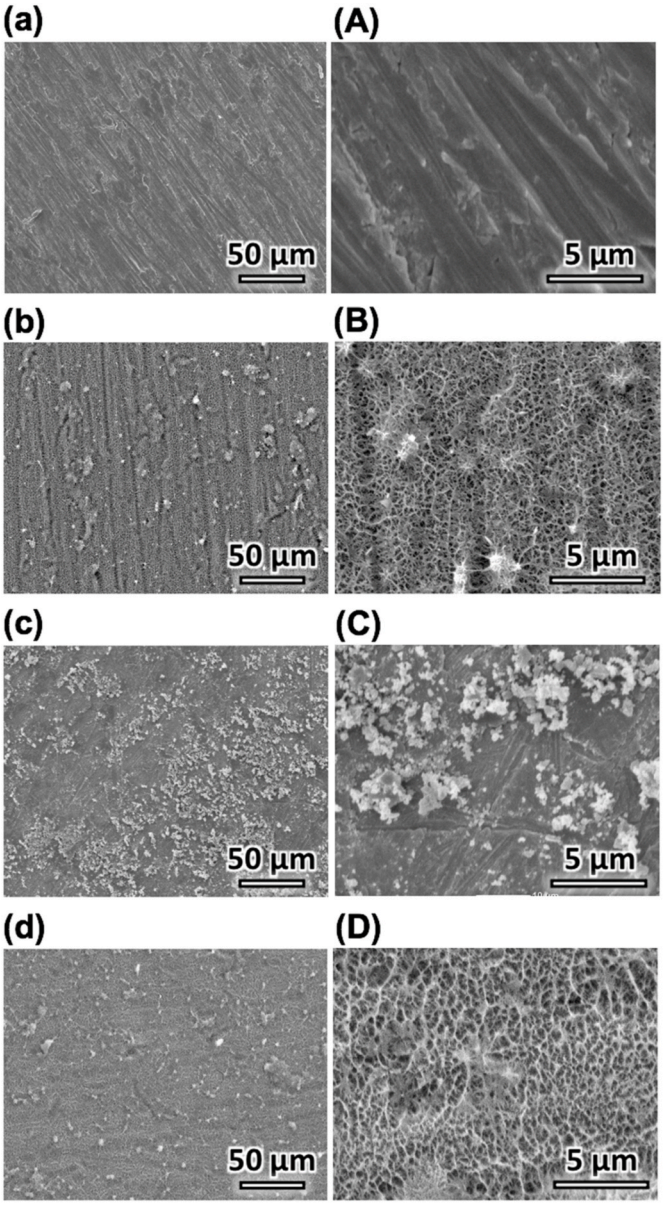

Fig. 2. SEM micrographs of the untreated and treated substrates: Ti (a, A), Ti-A (b, B), Ti-BG (c, C), and Ti-A-BG (d, D).

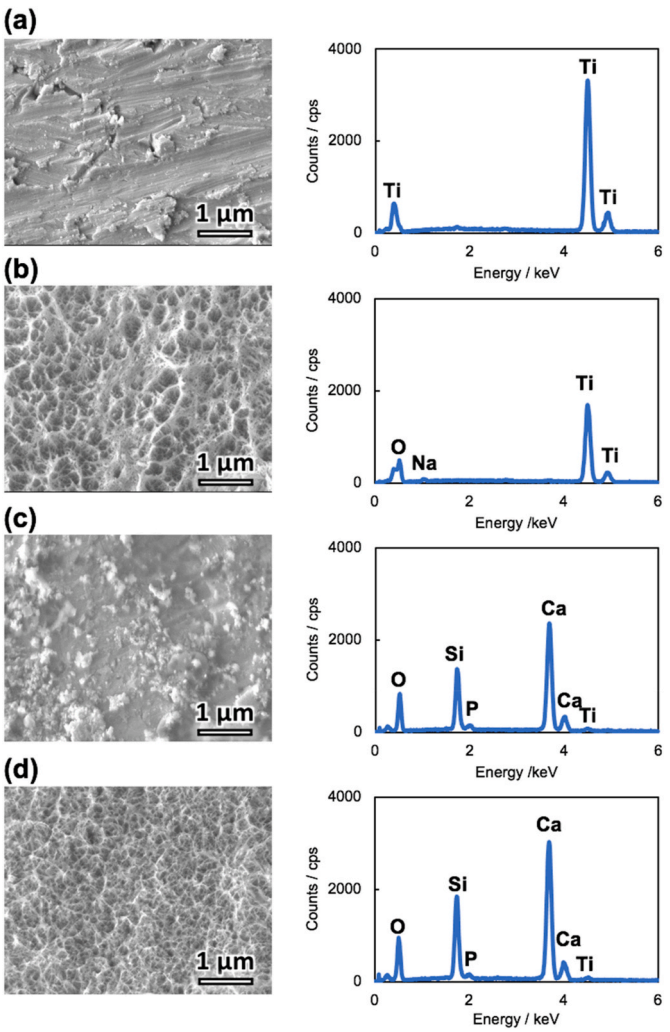

Fig. 3. FE-SEM micrographs and EDS spectra of the untreated and treated substrates: Ti (a), Ti-A (b), Ti-BG (c), and Ti-A-BG (d).

spectra. According to the EDS results, only the Ti peak was detected in the Ti sample elemental analysis. Fig. 3(b) exhibits the FE-SEM image and EDS spectra for the Ti-A substrate. A uniform, typical and fully covered porous nanostructure network layer was fabricated on the Ti surface. The EDS spectra results for the Ti-A sample confirmed that the treated surface containing Ti, O and Na elements resulted from the alkali treatment by the NaOH solution. Fig. 3(c) also shows that individual Ti-BG samples had no homogeneous distribution of the coating material (BG) on the substrate. However, the EDS spectra for the BG 58S coated surface presented Ca, P, and Si elements, which belonged to the BG 58S ceramic on the Ti substrate. Fig. 3(d) demonstrates the Ti-A-BG elemental analysis results. Based on the EDS spectra, the elements Ti, O, Ca, P and Si were detected on the Ti-A-BG substrate due to the hybridized treatment by the NaOH solution and the BG sol. The FE-SEM image also revealed an excellent fully-covered typical coating layer on the Ti-A-BG sample.

Fig. 4 shows the XRD patterns of the Ti substrates before and after treatment in various conditions. The Ti peak was assigned to Ti (Fig. 4 (a)) and Ti-A, Ti-BG, and Ti-A-BG substrates (Fig. 4(b, c), and d). The detected main peak for the Ti-A substrate's XRD pattern (Fig. 4(b)) was attributed to the titanate nanostructure network layer. The XRD pattern for the Ti-BG substrate (Fig. 4(c)) demonstrated that after BG 58S coating, the apatite peaks were detected in the pattern. The XRD pattern for Ti-A-BG (Fig. 4(d)), under the combined coating condition, confirmed the existence of the apatite phase on the substrate.

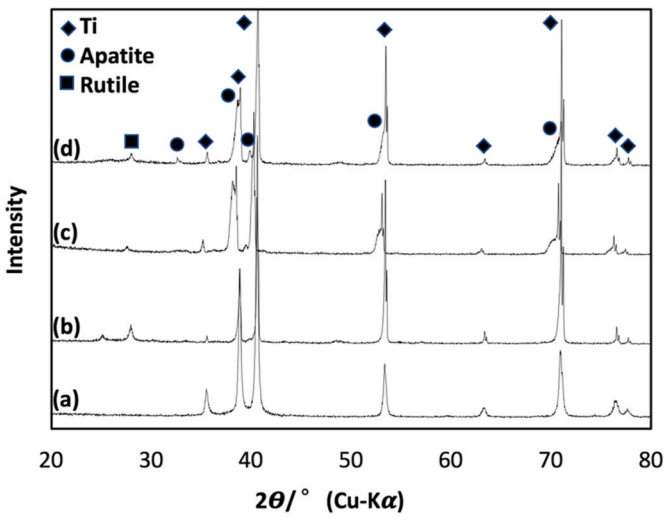

Fig. 4. XRD patterns of the unmodified and various modified Ti surfaces: Ti (a), Ti-A (b), Ti-BG (c), and Ti-A-BG (d).

3.2. Adhesive strength of the modified substrates

Fig. 5 exhibits the adhesion test results for the Ti substrates before and after treatment in different conditions. The measured adhesive strength for the Ti, Ti-A, Ti-BG, and Ti-A-BG substrates was 56.3 ± 8.9, 50.0 ± 6.3, 32.8 ± 3.0, and 45.4 ± 5.8 MPa, respectively. As shown in Fig. 5, the bond strength of the Ti-A sample was decreased slightly, as compared to Ti, without any significant difference. Also, there was a significant difference between Ti-A and Ti-BG in terms of adhesive strength. Both Ti-BG and Ti-A-BG substrates showed lower adhesive strength in comparison Ti and Ti-A ones. However, the bond strength of Ti-A-BG was not much low, as compared to Ti and Ti-A. Above all, the adhesive strength of the Ti-A-BG sample was significantly higher than that of Ti-BG sample.

Fig. 6 shows the FE-SEM micrographs and EDS results of the failure area for Ti, Ti-A, Ti-BG and Ti-A-BG after the adhesion test. The FE-SEM images exhibited that the resin adhering to the coated samples' surface partially remained on the surface, even after the adhesion test. According to the FE-SEM images for the BG-coated samples, Ti-BG and Ti-A-BG, the failure mechanism for the coatings was the mixed one. In other words, a mixture of adhesive and cohesive failures was shown on the coated samples. Besides, the EDS results for Ti-BG and Ti-A-BG, as obtained from the failure area, confirmed that after the adhesion test, all elements of the BG 58S coating, such as Ca, P, and Si, remained on the surface, even after the adhesion test.

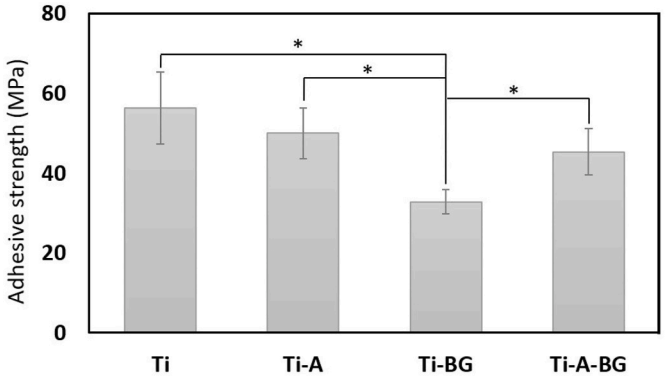

Fig. 5. The adhesive strength of the Ti, Ti-A, Ti-BG, and Ti-A-BG substrates. (*$p < 0.05$).

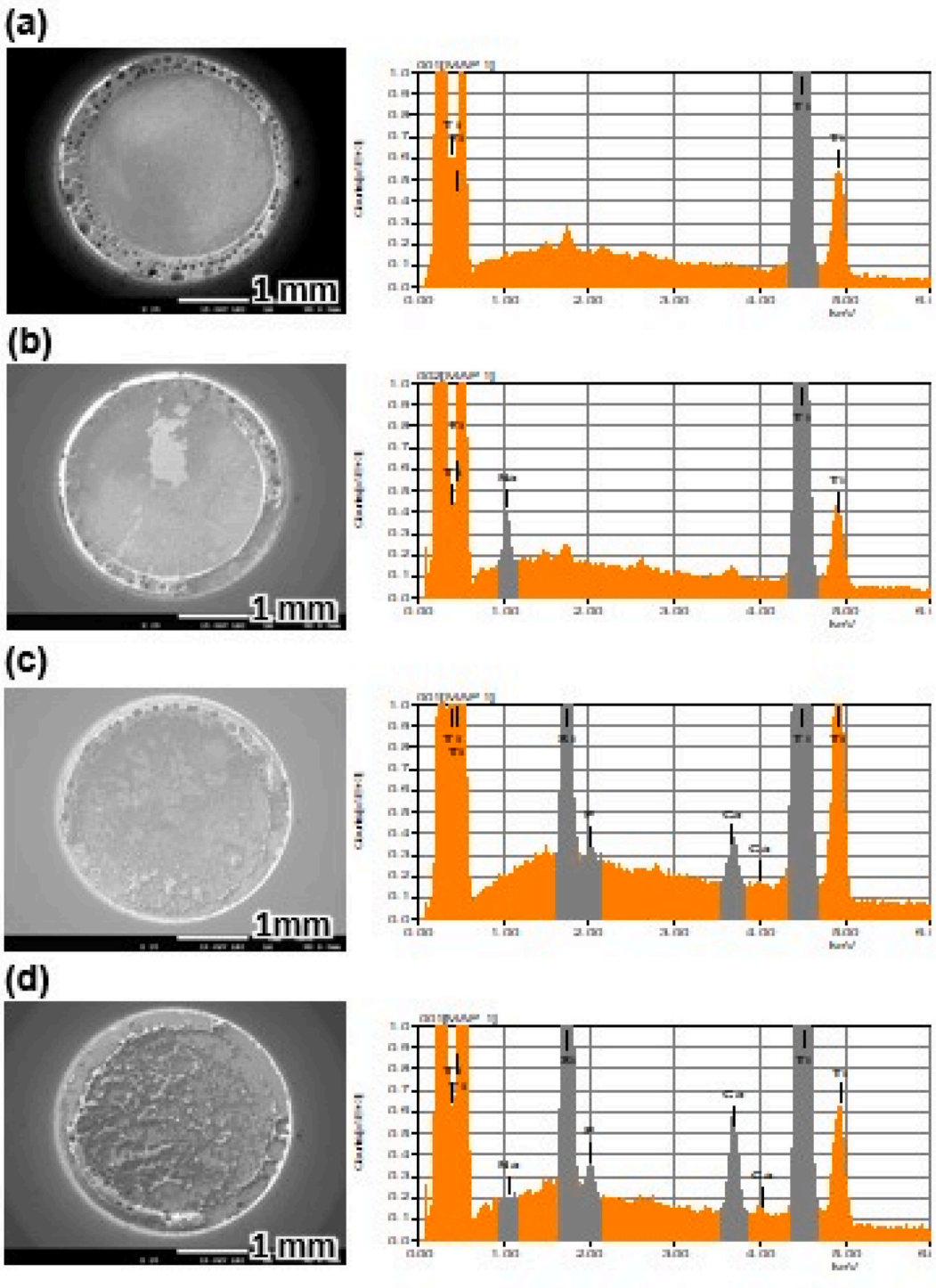

Fig. 6. FE-SEM and EDS results of the samples after the adhesion test: Ti (a), Ti-A (b), Ti-BG (c), and Ti-A-BG (d).

3.3. Cell response

Fig. 7 demonstrates the results of the viability test, as assessed by the MTS assay, and the effect on the cultured osteoblastic MC3T3-E1 cells in terms of the optical density (O.D.) of the proliferating cells for the unmodified Ti substrate and various modified substrates. As can be seen in Fig. 7, after 2 days of cells incubation, all samples' surfaces displayed biocompatible behaviors from their substrates, with no significant difference in their O.D. values. The viability test results also indicated the cytocompatibility of all unmodified and modified substrates from 2 to 4 days was as follows: Ti-A-BG > Ti-BG > Ti > Ti-A. However, as expected, from 4 to 6 days and after that, MC3T3-E1 cells on the surface were subjected to a combined alkali-BG treatment, and Ti-A-BG proliferated significantly, as compared to the untreated Ti surface as the control and the individually treated Ti-A surface.

Fig. 8 shows the results of the cell differentiation carried out by the ALP assay using the MC3T3-E1 cells, in terms of the O.D. of the differentiating cells for the unmodified Ti surface as the control and various modified Ti substrates. The results demonstrated that from 3 to 7 days of incubation, all specimens displayed approximately similar bioactivity

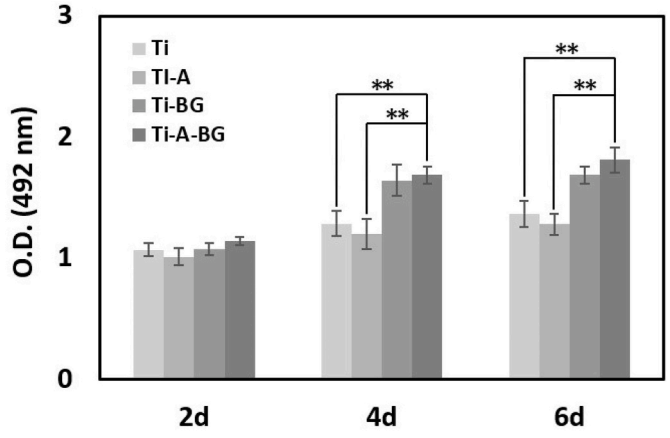

Fig. 7. The proliferation of MC3T3-E1 cultured on the Ti, Ti-A, Ti-BG, and Ti-A-BG substrates for 2, 4, and 6 days of incubation. (**p < 0.01).

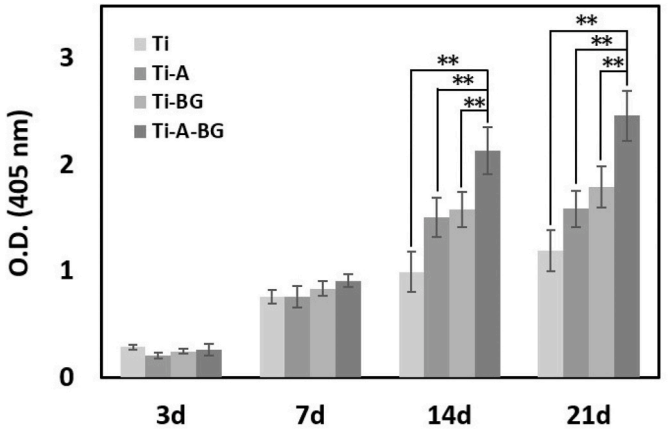

Fig. 8. The differentiation of MC3T3-E1 cultured on the Ti, Ti-A, Ti-BG, and Ti-A-BG substrates for 3, 7, 14, and 21 days of incubation. (**p < 0.01).

behaviors from their surfaces, with no considerable difference in their O.D. values. In other words, the cells could be differentiated on all unmodified and modified Ti substrates. However, according to Fig. 8, after 14 days of incubation, the MC3T3-E1 cells on the Ti-A-BG substrate presented the highest cell differentiation capacity with a significant difference between all unmodified and other modified substrates.

Fig. 9 demonstrates the biomineralization of the MC3T3-E1 cells on the Ti, Ti-A, Ti-BG, and Ti-A-BG samples after 3, 7, 14 and 21 days of incubation. As shown, from 3 to 21 days, with the progress of the experimental periods, according to the dark red stained area created after the Alizarin test, the highest mineralized matrix was observed on the Ti-A-BG sample among all others.

4. Discussion

4.1. Coating on the Ti

The coating was successfully formed on the Ti samples as it was expected. The obtained morphological information by SEM for the Ti-A treated samples proved that the alkali treatment produced a porous nanostructure coating layer on the Ti substrate; this was similar to the previous studies (HM Kim et al., 1997); (Kokubo and Yamaguchi, 2010). Based on our previous study, regarding Ti-BG treated samples, a relatively non-homogeneous distribution of the BG particles and the non-fully covered surface occurred after the modification procedure (Safaee et al., 2021). However, the surface morphology of the combined treated substrate, Ti-A-BG, proved a fully covered homogeneous BG coating layer with the regular distribution of the BG 58S nanoparticles on the porous nanostructure network. Moreover, the elemental analysis results indicated the existence of the Ca, P, and Si elements on the Ti-A-BG substrates similar to Ti-BG samples. The detected peak in the XRD patterns of the Ti-A sample referred to the titanate nanoporous layer, which was similar to the previous report (HM Kim et al., 1997). The apatite peaks identified in the XRD patterns of the Ti-BG sample had already been confirmed in the previous study (Li et al., 1991; Safaee et al., 2021). In the field of biomaterials science, with BG, the bioactivity of a material usually means that the material is capable of forming the apatite mineral on its surface (Vallittu et al., 2018). In the present study, the XRD peaks confirmed that this fundamental phenomenon had occurred indefinitely. Based on the comparison of the diffraction peaks for Ti-BG and Ti-A-BG in the XRD patterns, the apatite peak illustrated higher intensities for the Ti-A-BG rather than Ti-BG substrate after it being subjected to heat. The increasing rise in the intensity of the apatite peak, shown in the Ti-A-BG XRD pattern, could be due to the penetration of BG 58S into the porous nanostructure network and increasing of the apatite transformation amount which is limited due to the inadequate phosphorus ion level in BG.

4.2. Mechanical properties of the coating layer

In implantation, a strong adhesion must be established between the coated layer and the implant surface to prevent post-implant destruction (Mohseni et al., 2014; Wang et al., 1996). Even though the Ti-BG substrate's adhesive strength was the lowest among all samples, the measured adhesive strength for the Ti-BG sample, 32.8 ± 3.0 MPa, was greater than the adhesive strength of hydroxyapatite coating on the Ti surface, which was reported before (Arcos and Vallet-Regí, 2020). The bonding strength of the Ti-A-BG sample showed a significant difference in comparison to the Ti-BG substrate. In addition, according to the fractured area of the Ti-A-BG specimen, as shown in the FE-SEM images (Fig. 6(d)), and the existence of Ca, P, and Si on the combined treated surface, even after adhesion testing based on the EDS results (Fig. 6(d)), the coating failure mechanism was found to be a mixed one. That is, a mixture of adhesive and cohesive failures occurred on the combined treated specimens. Fiber-reinforced bioglass ceramics have the potential to be used as the load-bearing implants (Zhao et al., 2009). Fabrication of a fiber nano-level structure by alkali treatment on the Ti-A substrate therefore plays a key role in maintaining the reduction of bond strength, as proved by the adhesive strength results of the Ti-A samples in the literature (Lee et al., 2002). Also, according to the BG 58S fabrication protocol and alkali treatment method, there is an identical stage in the protocols of both methods. Since both techniques need to be heated at 650 °C, the titanium oxide phase could be formed on the Ti substrate after subjected to heat treatment. The phase transformation from anatase to rutile at 650 °C has been reported previously (Khodaei et al., 2017). Besides this, heat treatment at 650 °C as a final step of alkali treatment has shown to enhances bone bonding and improves the biological activity of the treated Ti surface (Nishiguchi et al., 1999). Also, heating at 650 °C as a final step of the BG preparation protocol is a necessity or a requirement that is needed. This common stage (heating at 650 °C) could contribute to the rise of BG and Ti substrate adhesion without collapsing after implantation. The originality of the current study in regard to biomechanical properties is the fabrication of a combined coating layer, including BG 58S nanoparticles, into a rough nanostructure network with a unique bonding strength behavior based on its nano level roughness. The measured adhesive strength for the Ti-A-BG sample proved that the BG 58S particles had adhered firmly to the Ti surface after subjected to alkali treatment. The measured adhesive strength for the Ti-A-BG samples in this study was higher than that of the bioactive borate glass coating on the Ti surface (36 ± 2 MPa) (Peddi et al., 2008).

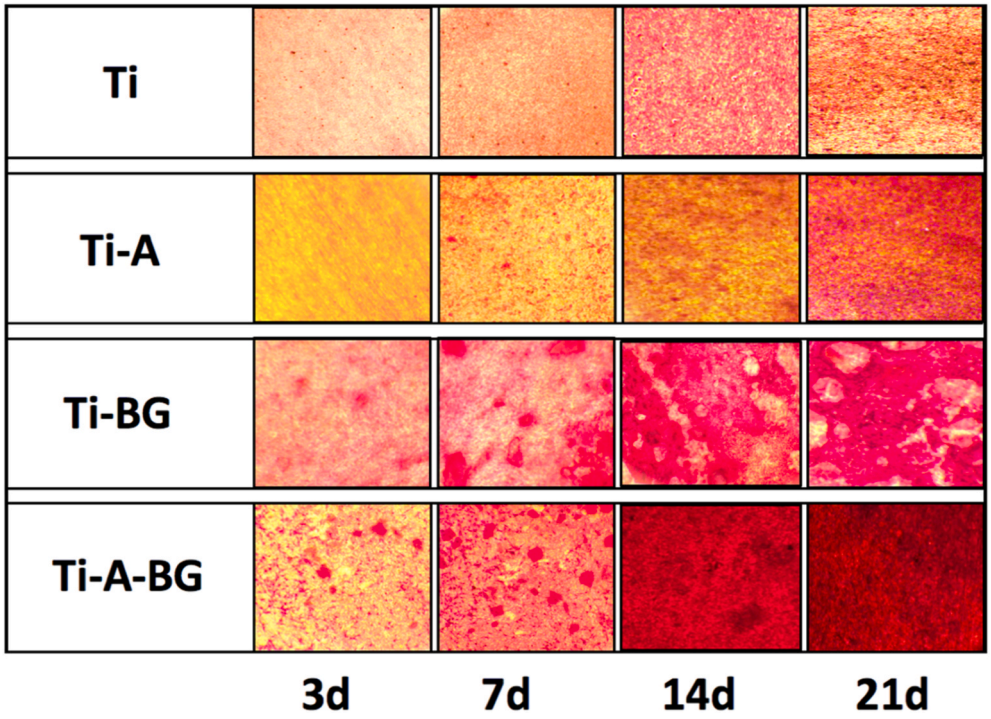

Fig. 9. Calcium nodules formed by the MC3T3-E1 cells cultured on Ti, Ti-A, Ti-BG, and Ti-A-BG upon 3, 7, 14 and 21 days of the incubation time.

4.3. Cell response

The cell proliferation data, as shown in Fig. 7, confirmed the biocompatibility of the Ti substrate due to its initial phases of cell proliferation. After BG 58S coating on the Ti substrate, the optimal cell proliferation ability of the BG 58S bioceramics (Gong et al., 2012); (Bielby et al., 2004) could guarantees the enhanced cell viability on Ti-BG, in comparison to the control group (Ti). The cell proliferation capacity of Ti, Ti-A and Ti-BG has already been assessed by scientists. However, the cell viability of the present hybrid modified substrate utilizing alkali-BG has not been previously investigated. As shown in Fig. 7, after 4 days of incubation, MC3T3-E1 cells on the Ti-A-BG modified surface proliferated significantly, as compared to Ti and Ti-A; also, there was a slight rise in its O.D. values compared to that of the Ti-BG substrate. Ti-A-BG samples for all cultured duration periods showed higher cell proliferation levels than that of the Ti-BG substrates; therefore, the cause of it being present could possibly be due to the homogeneous distribution of the BG 58S nanoparticles into the nanostructure network alkali treated sample after BG coating (Ti-A-BG). Finally, the cell viability study proposed that the BG 58S coating on the alkali treated Ti substrate led to the proper cell growth and proliferation environment. Furthermore, due to the alkali treatment process, the Ti sample should be soaked into the alkali solution, resulting in a titanate layer on its substrate. This layer has a good potential for easy and quick hydrolysis, leaving more hydroxyl groups on the modified Ti substrate, in comparison to the unmodified Ti substrate. Heating is the final step of the alkali treatment procedure causing the fabrication of a stable titania layer on the treated surface (H-M Kim et al., 1997). This procedure is necessary to trigger the nucleation of apatite (Li et al., 1994; Kitsugi et al., 1996) after BG coating. Therefore, the apatite transformation ability of the coated BG on the Ti surface could have a direct effect on the cell differentiation after 3 days based on Fig. 8 and the previous studies (Nishio et al., 2000). Regarding the Ti-BG substrate, the appropriate bioactivity and cell differentiation capability of the BG 58S ceramics (Gong et al., 2012) could guarantee enhanced cell osteoblastic differentiation, as compared to that of the control. In addition, BG stimulate bone regeneration, which is attributed to their dissolution products, stimulating cells at the genetic level (Jones et al., 2016). According to Fig. 8, due to the O.D. values, after 7 days of incubation, the Ti-BG treated substrate demonstrated less inhibition of the ALP activity of MC3T3-E1 cells in comparison to Ti and Ti-A samples (Moritz et al., 2004a). The reason being for this could be due to the existence of Ca and P elements, as confirmed by EDS, which would improve cell differentiation (Olmo et al., 2003). As can be seen in Fig. 8, from the data obtained, after 14 days of incubation of MC3T3-E1 cells on the combined Alkali-BG substrate, Ti-A-BG, differentiated significantly in comparison to Ti, Ti-A and Ti-BG, thus suggesting that the combined treated system is more suitable than the untreated and any other treated surfaces. The Alizarin red S staining method is a popular method to investigate the biomineralization level of MC3T3-E1 cells (Gregory et al., 2004). As can be seen in Fig. 9, after 14 d of incubation, the calcium nodules formation of the cells on the Ti-A-BG sample was raised, as compared to Ti-BG. This elevation was proportional to the escalation of Ca and P on the surface, as indicated by EDS and a previous study (El-Ghannam et al., 1997). On the other hand, as can be seen in Figs. 2 and 3, Ti surface was ranked from ground (Ti) to porousness after alkali treatment (Ti-A). This can certainly escalate the area level and increase nano-topographical features per unit area (Bsat et al., 2015). In the Ti-A-BG hybridized application, after placing the BG sol into the porous nanonetwork structure of Ti-A, the growth in the area caused further rise of the Ca and P release from the surface.

Finally, according to all assessments and the data gained for the combined alkali-BG modified substrate, it could be claimed that the Ti-A-BG treated surface benefited from all advantageous effects brought on by both the alkali treatment and BG coating. They intensified and increased the beneficial factors by improving the quality value of each other's advantages and at the same time, companesated for their disadvantages. The combined application of alkali treatment and BG coating is presented as a promising surface chemical modification method for the implant industry. Besides this, the study demonstrated the key role of surface roughness in optimizing the typical coating on the Ti surface which enhanced the mechanical and biological properties. Further study is, however, recommended to probe the mechanism of the effect of the combined alkali-BG treatment on the Ti implants surface.

5. Conclusion

Ti substrate was successfully coated through alkali treatment followed by the adding of the BG 58S Sol to the alkali treatment solution. Characterization results confirmed the existence of Ca and P elements and apatite phase transformation ability resulting from the BG 58S coating and a porous nanostructure layer caused by alkali treatment on the combined Ti-A-BG surface.

The measured adhesive strength for the combined Ti-A-BG substrate's surface proved the high bonding strength between the coating and Ti substrate. The hybrid Alkali-BG coating improved the cell proliferation, ALP activity and bone nodule formation of the Ti substrate, exhibiting the best performance among all other substrates in terms of biological properties.

CRediT authorship contribution statement

Mahdis Nesabi: Planned the experiments. Collected and analyzed the data. Wrote the manuscript.Alireza Valanezhad: Presented the idea. Mentored for methodology and data analysis. Wrote the manuscript. Sirus Safaee: Analyzed the data. Wrote the manuscript.Tetsurou Odatsu: Performed the cell study and data analysis.Shigeaki Abe: Wrote the manuscript.Ikuya Watanabe: Supervised the team and wrote the manuscript.

Declaration of competing interest

The authors declare that they have no known competing financial interests or personal relationships that could have appeared to influence the work reported in this paper.

Acknowledgments

This study was supported by Grant-in-Aid (No. 19K10250 and No.18K09686) from Scientific Research of the Japan Society for the Promotion of Science (JSPS).

References

Arcos, D., Vallet-Regí, M., 2020. Substituted hydroxyapatite coatings of bone implants. J. Mater. Chem. B 8, 1781–1800.
Bielby, R.C., Christodoulou, I.S., Pryce, R.S., Radford, W.J., Hench, L.L., Polak, J.M., 2004. Time-and concentration-dependent effects of dissolution products of 58S sol–gel bioactive glass on proliferation and differentiation of murine and human osteoblasts. Tissue Eng. 10, 1018–1026.
Bsat, S., Yavari, S.A., Munsch, M., Valstar, E.R., Zadpoor, A.A., 2015. Effect of alkali-acid-heat chemical surface treatment on electron beam melted porous titanium and its apatite forming ability. Materials 8, 1612–1625.
Bui, X.V., Dang, T.H., 2019. Bioactive glass 58S prepared using an innovation sol-gel process. Process. Appl. Ceram 13, 98–103.
Camargo, W.A., Takemoto, S., Hoekstra, J.W., Leeuwenburgh, S.C.G., Jansen, J.A., van den Beucken, J.J.J.P., Alghamdi, H.S., 2017. Effect of surface alkali-based treatment of titanium implants on ability to promote in vitro mineralization and in vivo bone formation. Acta Biomater. 57, 511–523. https://doi.org/10.1016/j.actbio.2017.05.016.
Chen, J., Zeng, L., Chen, X., Liao, T., Zheng, J., 2018. Preparation and characterization of bioactive glass tablets and evaluation of bioactivity and cytotoxicity in vitro. Bioact. Mater 3, 315–321.
Conforto, E., Caillard, D., Mueller, L., Müller, F., 2008. The structure of titanate nanobelts used as seeds for the nucleation of hydroxyapatite at the surface of titanium implants. Acta Biomater. 4, 1934–1943.
Davies, J.E., Ajami, E., Moineddin, R., Mendes, V.C., 2013. The roles of different scale ranges of surface implant topography on the stability of the bone/implant interface. Biomaterials 34, 3535–3546.
El-Ghannam, A., Ducheyne, P., Shapiro, I., 1997. Formation of surface reaction products on bioactive glass and their effects on the expression of the osteoblastic phenotype and the deposition of mineralized extracellular matrix. Biomaterials 18, 295–303.
Geetha, M., Singh, A.K., Asokamani, R., Gogia, A.K., 2009. Ti based biomaterials, the ultimate choice for orthopaedic implants–a review. Prog. Mater. Sci. 54, 397–425.
Gentleman, E., Fredholm, Y.C., Jell, G., Lotfibakhshaiesh, N., O'Donnell, M.D., Hill, R.G., Stevens, M.M., 2010. The effects of strontium-substituted bioactive glasses on osteoblasts and osteoclasts in vitro. Biomaterials 31, 3949–3956.
Gepreel, M.A.-H., Niinomi, M., 2013. Biocompatibility of Ti-alloys for long-term implantation. J. Mech. Behav. Biomed. Mater 20, 407–415.
Gittens, R.A., McLachlan, T., Olivares-Navarrete, R., Cai, Y., Berner, S., Tannenbaum, R., Schwartz, Z., Sandhage, K.H., Boyan, B.D., 2011. The effects of combined micron-/submicron-scale surface roughness and nanoscale features on cell proliferation and differentiation. Biomaterials 32, 3395–3403.
Gong, W.Y., Dong, Y.M., Chen, X.F., Karabucak, B., 2012. Nano-sized 58S bioactive glass enhances proliferation and osteogenic genes expression of osteoblast-like cells. Chin. J. Dent. Res. 15, 145.
Gregory, C.A., Gunn, W.G., Peister, A., Prockop, D.J., 2004. An Alizarin red-based assay of mineralization by adherent cells in culture: comparison with cetylpyridinium chloride extraction. Anal. Biochem. 329, 77–84.
He, F., Yang, G., Wang, X., Zhao, S., 2009. Bone responses to rough titanium implants coated with biomimetic Ca-P in rabbit tibia. J. Biomed. Mater. Res. Part B Appl. Biomater. Off. J. Soc. Biomater. Jpn. Soc. Biomater. Aust. Soc. Biomater. Korean Soc. Biomater 90, 857–863.
Hench, L.L., Splinter, R.J., Allen, W., Greenlee, T., 1971. Bonding mechanisms at the interface of ceramic prosthetic materials. J. Biomed. Mater. Res. 5, 117–141.
Houreh, A.B., Labbaf, S., Ting, H.-K., Ejeian, F., Jones, J.R., Esfahani, M.-H.N., 2017. Influence of calcium and phosphorus release from bioactive glasses on viability and differentiation of dental pulp stem cells. J. Mater. Sci. 52, 8928–8941.
Jones, J.R., Brauer, D.S., Hupa, L., Greenspan, D.C., 2016. Bioglass and bioactive glasses and their impact on healthcare. Int. J. Appl. Glass Sci. 7, 423–434.
Khodaei, M., Valanezhad, A., Watanabe, I., Yousefi, R., 2017. Surface and mechanical properties of modified porous titanium scaffold. Surf. Coating. Technol. 315, 61–66.
Khorasani, A.M., Goldberg, M., Doeven, E.H., Littlefair, G., 2015. Titanium in biomedical applications—properties and fabrication: a review. J. Biomater. Tissue Eng 5, 593–619.
Kim, H.M., Miyaji, F., Kokubo, T., Nakamura, T., 1997. Effect of heat treatment on apatite-forming ability of Ti metal induced by alkali treatment. J. Mater. Sci. Mater. Med. 8, 341–347.
Kim, H.-M., Miyaji, F., Kokubo, T., Nakamura, T., 1997. Bonding strength of bonelike apatite layer to Ti metal substrate. J. Biomed. Mater. Res. 38, 121–127.
Kitsugi, T., Nakamura, T., Oka, M., Yan, W., Goto, T., Shibuya, T., Kokubo, T., Miyaji, S., 1996. Bone bonding behavior of titanium and its alloys when coated with titanium oxide (TiO2) and titanium silicate (Ti5Si3). J. Biomed. Mater. Res. Off. J. Soc. Biomater. Jpn. Soc. Biomater 32, 149–156.
Kokubo, T., Yamaguchi, S., 2010. Bioactive Ti metal and its alloys prepared by chemical treatments: state-of-the-art and future trends. Adv. Eng. Mater. 12, B579–B591.
Le Guéhennec, L., Soueidan, A., Layrolle, P., Amouriq, Y., 2007. Surface treatments of titanium dental implants for rapid osseointegration. Dent. Mater. 23, 844–854.
Lee, B., Do Kim, Y., Shin, J.H., Hwan Lee, K., 2002. Surface modification by alkali and heat treatments in titanium alloys. J. Biomed. Mater. Res. Off. J. Soc. Biomater. Jpn. Soc. Biomater. Aust. Soc. Biomater. Korean Soc. Biomater 61, 466–473.
Li, J., Wang, G., Wang, D., Wu, Q., Jiang, X., Liu, X., 2014. Alkali-treated titanium selectively regulating biological behaviors of bacteria, cancer cells and mesenchymal stem cells. J. Colloid Interface Sci. 436, 160–170.
Li, P., Ohtsuki, C., Kokubo, T., Nakanishi, K., Soga, N., de Groot, K., 1994. The role of hydrated silica, titania, and alumina in inducing apatite on implants. J. Biomed. Mater. Res. 28, 7–15.
Li, R., Clark, A., Hench, L., 1991. An investigation of bioactive glass powders by sol-gel processing. J. Appl. Biomater. 2, 231–239.
Liu, X., Chu, P.K., Ding, C., 2004. Surface modification of titanium, titanium alloys, and related materials for biomedical applications. Mater. Sci. Eng. R Rep. 47, 49–121.
Mendes, V.C., Moineddin, R., Davies, J.E., 2007. The effect of discrete calcium phosphate nanocrystals on bone-bonding to titanium surfaces. Biomaterials 28, 4748–4755.
Mendonça, G., Mendonça, D.B., Aragao, F.J., Cooper, L.F., 2008. Advancing dental implant surface technology–from micron-to nanotopography. Biomaterials 29, 3822–3835.
Moghanian, A., Koohfar, A., Hosseini, S., Hosseini, S.H., Ghorbanoghli, A., Sajjadnejad, M., Raz, M., Elsa, M., Sharifianjazi, F., 2021a. Synthesis, characterization and in vitro biological properties of simultaneous co-substituted Ti + 4/Li+ 1 58s bioactive glass. J. Non-Cryst. Solids 561, 120740.
Moghanian, A., Nasiripour, S., Hosseini, S.M., Hosseini, S.H., Rashvand, A., Ghorbanoghli, A., Pazhouheshgar, A., Jazi, F.S., 2021b. The effect of Ag substitution on physico-chemical and biological properties of sol-gel derived 60% SiO2-31% CaO-4% P2O5-5% TiO2 (mol%) quaternary bioactive glass. J. Non-Cryst. Solids 560, 120732.
Moghanian, A., Nasiripour, S., Koohfar, A., Sajjadnejad, M., Hosseini, S., Taherkhani, M., Miri, Z., Hosseini, S.H., Aminitabar, M., Rashvand, A., 2021c. Characterization, in vitro bioactivity and biological studies of sol-gel-derived TiO2 substituted 58S bioactive glass. Int. J. Appl. Ceram. Technol. 18, 1430–1441.
Moghanian, A., Nasiripour, S., Miri, Z., Hajifathali, Z., Hosseini, S.H., Sajjadnejad, M., Aghabarari, R., Nankali, N., Miri, A.K., Tahriri, M., 2021d. Structural and in vitro biological evaluation of sol-gel derived multifunctional Ti+ 4/Sr+ 2 co-doped bioactive glass with enhanced properties for bone healing. Ceram. Int. 47, 29451–29462.
Moghanian, A., Zohourfazeli, M., Tajer, M.H.M., Miri, Z., Hosseini, S., Rashvand, A., 2021e. Preparation, characterization and in vitro biological response of simultaneous co-substitution of Zr+ 4/Sr+ 2 58S bioactive glass powder. Ceram. Int. 47, 23762–23769.
Mohseni, E., Zalnezhad, E., Bushroa, A.R., 2014. Comparative investigation on the adhesion of hydroxyapatite coating on Ti–6Al–4V implant: a review paper. Int. J. Adhes. Adhes 48, 238–257. https://doi.org/10.1016/j.ijadhadh.2013.09.030.
Moritz, N., Rossi, S., Vedel, E., Tirri, T., Ylänen, H., Aro, H., Närhi, T., 2004a. Implants coated with bioactive glass by CO 2-laser, an in vivo study. J. Mater. Sci. Mater. Med. 15, 795–802.

Moritz, N., Vedel, E., Ylänen, H., Jokinen, M., Hupa, M., Yli-Urpo, A., 2004b. Characterisation of bioactive glass coatings on titanium substrates produced using a CO 2 laser. J. Mater. Sci. Mater. Med. 15, 787–794.

Nishiguchi, S., Nakamura, T., Kobayashi, M., Kim, H.-M., Miyaji, F., Kokubo, T., 1999. The effect of heat treatment on bone-bonding ability of alkali-treated titanium. Biomaterials 20, 491–500. https://doi.org/10.1016/S0142-9612(98)90203-4.

Nishio, K., Neo, M., Akiyama, H., Nishiguchi, S., Kim, H., Kokubo, T., Nakamura, T., 2000. The effect of alkali-and heat-treated titanium and apatite-formed titanium on osteoblastic differentiation of bone marrow cells. J. Biomed. Mater. Res. 52, 652–661.

Olmo, N., Martín, A.I., Salinas, A.J., Turnay, J., Vallet-Regí, M., Lizarbe, M.A., 2003. Bioactive sol–gel glasses with and without a hydroxycarbonate apatite layer as substrates for osteoblast cell adhesion and proliferation. Biomaterials 24, 3383–3393.

Oshida, Y., 2010. Bioscience and Bioengineering of Titanium Materials. Elsevier.

Peddi, L., Brow, R.K., Brown, R.F., 2008. Bioactive borate glass coatings for titanium alloys. J. Mater. Sci. Mater. Med. 19, 3145–3152.

Ponsonnet, L., Reybier, K., Jaffrezic, N., Comte, V., Lagneau, C., Lissac, M., Martelet, C., 2003. Relationship between surface properties (roughness, wettability) of titanium and titanium alloys and cell behaviour. Mater. Sci. Eng. C 23, 551–560.

Rahmani, M., Moghanian, A., Yazdi, M.S., 2021. The effect of Ag substitution on physicochemical and biological properties of sol-gel derived 60% SiO2–31% CaO–4% P2O5–5% Li2O (mol%) quaternary bioactive glass. Ceram. Bar Int. 47, 15985–15994.

Ren, K., Dusad, A., Zhang, Y., Wang, D., 2013. Therapeutic intervention for wear debris-induced aseptic implant loosening. Acta Pharm. Singapore Bus. 3, 76–85.

Saatchi, A., Arani, A.R., Moghanian, A., Mozafari, M., 2021. Cerium-doped bioactive glass-loaded chitosan/polyethylene oxide nanofiber with elevated antibacterial properties as a potential wound dressing. Ceram. Int. 47, 9447–9461.

Safaee, S., Valanezhad, A., Nesabi, M., Jafarnia, S., Sano, H., Shahabi, S., Abe, S., Watanabe, I., 2021. Fabrication of bioactive glass coating on pure titanium by sol-dip method: dental applications. Dent. Mater. J. 2020, 323.

Schrooten, J., Helsen, J.A., 2000. Adhesion of bioactive glass coating to Ti6Al4V oral implant. Biomaterials 21, 1461–1469. https://doi.org/10.1016/S0142-9612(00)00027-2.

Singh, R., Dahotre, N.B., 2007. Corrosion degradation and prevention by surface modification of biometallic materials. J. Mater. Sci. Mater. Med. 18, 725–751.

Valanezhad, A., Tsuru, K., Maruta, M., Kawachi, G., Matsuya, S., Ishikawa, K., 2012. A new biocompatible coating layer applied on titanium substrates using a modified zinc phosphatizing method. Surf. Coat. Technol. 206, 2207–2212.

Vallittu, P.K., Boccaccini, A.R., Hupa, L., Watts, D.C., 2018. Bioactive dental materials-Do they exist and what does bioactivity mean?.

Wang, S., Lacefield, W.R., Lemons, J.E., 1996. Interfacial shear strength and histology of plasma sprayed and sintered hydroxyapatite implants in vivo. Biomaterials 17, 1965–1970.

Zhao, D., Moritz, N., Laurila, P., Mattila, R., Lassila, L., Strandberg, N., Mäntylä, T., Vallittu, P., Aro, H., 2009. Development of a multi-component fiber-reinforced composite implant for load-sharing conditions. Med. Eng. Phys. 31, 461–469.

Zohourfazeli, M., Tajer, M.H.M., Moghanian, A., 2021. Comprehensive investigation on multifunctional properties of zirconium and silver co-substituted 58S bioactive glass. Ceram. Int. 47, 2499–2507.